When does cyclic dominance lead to stable spiral waves?

Bartosz Szczesny,* Mauro Mobilia,† and Alastair M. Rucklidge‡
Department of Applied Mathematics, School of Mathematics, University of Leeds, Leeds LS2 9JT, U.K.
(Dated: 31 October 2012)

Species diversity in ecosystems is often accompanied by characteristic spatio-temporal patterns. Here, we consider a generic two-dimensional population model and study the spiraling patterns arising from the combined effects of cyclic dominance of three species, mutation, pair-exchange and individual hopping. The dynamics is characterized by nonlinear mobility and a Hopf bifurcation around which the system's four-phase state diagram is inferred from a complex Ginzburg-Landau equation derived using a perturbative multiscale expansion. While the dynamics is generally characterized by spiraling patterns, we show that spiral waves are stable in only one of the four phases. Furthermore, we characterize a phase where *nonlinearity* leads to the annihilation of spirals and to the spatially uniform dominance of each species in turn. Away from the Hopf bifurcation, when the coexistence fixed point is unstable, the spiraling patterns are also affected by the nonlinear diffusion.

PACS numbers: 87.23.Cc, 05.45.-a, 02.50.Ey, 87.18.Hf

In nature, organisms live in areas much larger than the distances they typically travel and thus interact with a finite number of individuals in their neighborhood. Space and mobility are therefore crucial ingredients to understand how populations evolve, and how ecosystems self-organize. They are often responsible for pattern formation, whose origin in ecosystems has been a subject of intense research for decades [1, 2]. In his pioneering work, Turing showed that pattern-forming instabilities can be caused by diffusion [3]. While Turing patterns have been found in ecology and biology [1], the requirements of Turing's theory (e.g. separation of scales in diffusivities) appear to be too restrictive to explain the formation of patterns in many ecosystems, see e.g. [4].

Another important problem concerns the mechanisms promoting the maintenance of biodiversity [5]. In this context, cyclic dominance has recently been proposed as an intriguing motif facilitating the coexistence of diverse species in ecosystems. Examples of cyclic competition between three species can be found in coral reef invertebrates, Californian lizards, and communities of *E.coli* [2, 6, 7]. In the experiments of Ref. [6], the cyclic competition of three bacterial strains on two-dimensional plates was shown to yield intricate patterns sustaining species coexistence. Such competition is metaphorically described by *rock-paper-scissors* (RPS) games, where "rock crushes scissors, scissors cut paper, and paper wraps rock" [8]. While non-spatial RPS-like models often evolve toward extinction of all but one species in finite time [9], their spatial counterparts are generally characterized by the long coexistence of species and by the formation of complex spatio-temporal patterns [10–14]. Recently, two-dimensional versions of a model introduced by May and Leonard [15] have received much attention [11–14]. When mobility is implemented by pair-exchange among neighbors, species coexistence is long-lived and populations form non-Turing spiraling patterns below a certain mobility threshold, whereas biodiversity is lost when that threshold is exceeded [11].

In this Letter, we characterize the intricate patterns emerging from the dynamics of a *generic* model of a cyclically competing three-species population, and study how these patterns affect the maintenance of biodiversity in two dimensions. The basic evolutionary processes considered are the most general form of cyclic dominance obtained by combining and unifying the interactions of Refs. [11, 12, 14, 16]. Inspired by the experiments of [7], the model is formulated at the metapopulation level [17], and is characterized by a Hopf bifurcation as well as by nonlinear mobility. While spiraling patterns have often been observed numerically in related models [11–14], we here demonstrate that nonlinearity and mobility can disrupt the stability of the ensuing spiral waves. Our main result is the state diagram derived from a *controlled* multiscale expansion around the Hopf bifurcation's onset and characterized by three phases in which spiral waves are *unstable*, and by one phase where spiraling patterns are stable. This implies the existence of a region of the parameter space where spiral waves annihilate and each species dominates the system in turn.

The generic model of cyclic competition is defined as a periodic square lattice of L^2 patches (L being the linear size) labeled by a vector $\boldsymbol{l} = (l_1, l_2)$ [18]. Each patch has a limited carrying capacity, accommodating at most N individuals, and consists of a well-mixed population of species S_1, S_2, S_3 and empty spaces $\emptyset$. Within each patch $\boldsymbol{l}$, the population composition evolves according to

$$S_i + S_{i+1} \xrightarrow{\sigma} S_i + \emptyset \qquad S_i + S_{i+1} \xrightarrow{\zeta} 2S_i \tag{1}$$

$$S_i + \emptyset \xrightarrow{\beta} 2S_i \qquad S_i \xrightarrow{\mu} S_{i\pm1}, \tag{2}$$

where the species index $i \in \{1, 2, 3\}$ is *ordered cyclically* such that $S_{3+1} \equiv S_1$ and $S_{1-1} \equiv S_3$. The reactions (1) describe the cyclic competition between the species: S_i dominates over S_{i+1} while being dominated by S_{i-1}. Here, we consider a generic form of cyclic competition by separating the zero-sum process of

dominance-replacement (rate ζ), as studied in Ref. [12], from the dominance-removal selection process (rate σ) of Refs. [11, 14]. With reactions (2), we assume that births (rate β) occur independently of the cyclic competition provided that space ($\emptyset$) is available, and that each species can mutate into another (rate μ).

As biological movement is often nonlinear and driven by local population density [19], we here *divorce* hopping (rate δ_D) from pair-exchanges (rate δ_E) between nearest-neighbor patches $\boldsymbol{l}$ and $\boldsymbol{l}'$, according to

$$\begin{aligned} [S_i]_{\boldsymbol{l}}[\emptyset]_{\boldsymbol{l}'} &\xrightarrow{\delta_D} [\emptyset]_{\boldsymbol{l}}[S_i]_{\boldsymbol{l}'} \\ [S_i]_{\boldsymbol{l}}[S_{i\pm1}]_{\boldsymbol{l}'} &\xrightarrow{\delta_E} [S_{i\pm1}]_{\boldsymbol{l}}[S_i]_{\boldsymbol{l}'}, \end{aligned} \tag{3}$$

where $\boldsymbol{l}$ and $\boldsymbol{l}'$ lie in 4-neighborhood. The processes (3) lead to nonlinear mobility (see (5) below) and allow us to distinguish the movement in crowded regions, where pair-exchange dominates, from mobility in dilute systems, where hopping is more likely. The metapopulation model (1)-(3) is well-suited to capture stochastic effects via size expansion in the carrying capacity and allows a natural connection with its deterministic description [4, 20, 21].

It has to be noted that most previous works considered lattice models with $N = 1$ and nearest-neighbor reactions (1)-(2), while here these interactions occur on-site. Apart from these differences, the processes that we consider are similar to those of [11] when $\zeta = \mu = 0$ and $\delta_D = \delta_E$, while some aspects of the system's properties with $\zeta \neq 0$, $\mu \neq 0$ and $\delta_D \neq \delta_E$ have been investigated in [12], [16] and [14], respectively.

When $N \to \infty$, the leading-order term in the size expansion yields mean field rate equations for the continuous species densities $s_i = N_{S_i}/N$. Here, N_{S_i} is the number of S_i's in one patch. With $\boldsymbol{s} \equiv (s_1, s_2, s_3)$,

$$\begin{aligned} \frac{ds_i}{dt} &= s_i[\beta(1-r) - \sigma s_{i-1} + \zeta(s_{i+1} - s_{i-1})] \\ &\quad +\mu(s_{i-1} + s_{i+1} - 2s_i) \equiv \mathcal{F}_i(\boldsymbol{s}), \end{aligned} \tag{4}$$

where $r \equiv s_1 + s_2 + s_3$ is the total density. Eqs. (4) admit a coexistence fixed point $\boldsymbol{s}^* = \frac{\beta}{3\beta+\sigma}(1,1,1)$. In the presence of mutations, $\boldsymbol{s}^*$ is an asymptotically stable focus when $\mu > \mu_H = \frac{\beta\sigma}{6(3\beta+\sigma)}$, while there is a supercritical Hopf bifurcation (HB) [16] at $\mu = \mu_H$ and a stable limit cycle of frequency $\omega_H \approx \frac{\sqrt{3\beta}(\sigma+2\zeta)}{2(3\beta+\sigma)}$ when $\mu < \mu_H$. For later convenience, the departure from the HB point is measured by a parameter ϵ defined by $\mu = \mu_H - \frac{1}{3}\epsilon^2$. In stark contrast, when $\mu = 0$ (no mutations), the coexistence state $\boldsymbol{s}^*$ is never asymptotically stable. Instead, solutions of (4) are either heteroclinic cycles ($\mu = 0$ and $\sigma > 0$) [15] or nested neutrally stable periodic orbits ($\mu = \sigma = 0$) [8]. In either case, finite-size fluctuations cause the rapid extinction of two of the three species in a non-spatial setting [9].

When spatial dependence is taken into account in the limit $L \to \infty$ and lattice spacing $\to 0$, the spatial coordinate $\boldsymbol{x} \equiv \boldsymbol{l}/L$ becomes continuous. The densities depend on space and time, $s_i \equiv s_i(\boldsymbol{x}, t)$, and obey

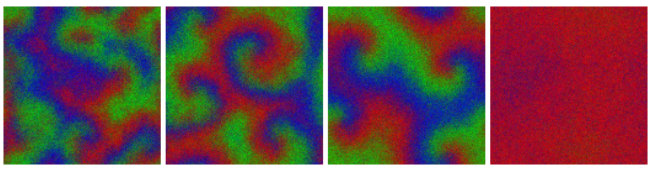

FIG. 1: Reactive steady states in stochastic simulations of reactions (1)-(3). Here, $L^2 = 128^2$, $N = 64$, $\beta = \sigma = \delta_D = \delta_E = 1$, $\mu = 0.02 < \mu_H = 0.042$ ($\epsilon = 0.25$) and, from left to right, $\zeta = (1.8, 1.2, 0.6, 0)$. Each pixel describes a patch with normalized RGB representation $(red, green, blue) = (s_1, s_2, s_3)$ of its state. The right-most panel shows an oscillatory homogeneous state in which each of the species dominates the whole population in turn (see Fig. 3 for time evolution). Initially $\boldsymbol{s} \approx \boldsymbol{s}^*$ with small random perturbations, see [18].

$$\partial_t s_i = \mathcal{F}_i(\boldsymbol{s}) + \delta_D \Delta s_i + (\delta_D - \delta_E)\left(s_i \Delta r - r \Delta s_i\right), \tag{5}$$

where $\Delta = \partial^2_{x_1} + \partial^2_{x_2}$ and the nonlinear diffusive terms $(s_i\Delta r - r\Delta s_i)$ arise from the divorce between pair-exchange and hopping. With our metapopulation approach, these partial differential equation (PDEs) can be derived in the continuum limit at the lowest order of a size expansion in N of the Markov chain associated with the processes (1)-(3) [4, 20].

We aim to unravel the combined influence of nonlinearity, mobility and noise on the system's dynamics and the formation and stability of coherent patterns. To gain some insight, we report some typical lattice simulations obtained in the regime where there is a limit cycle ($\mu < \mu_H$). As shown in Fig. 1, this regime is characterized by spiraling patterns found in four different phases, whereas we have found no patterns when $\mu > \mu_H$ (see [18]). We have checked that the PDEs (5) faithfully reproduce the behaviors obtained with lattice simulations as shown in Fig. 1. Our analysis is therefore based on (5), whose properties are conveniently discussed by performing the linear transformation $\boldsymbol{s} - \boldsymbol{s}^* \to (u, v, w)$, with $u = -(r + s_3)/\sqrt{6}$, $v = (s_2 - s_1)/\sqrt{2}$ and $w = r/\sqrt{3}$. In these variables, the linear part of (4) can be written in the Jordan normal form $\partial_t(u + iv) = (\epsilon^2 + i\omega_H)(u + iv)$ and $\partial_t w = -\beta w$.

To make analytical progress, we perform a space and time perturbation expansion in the parameter ϵ around the onset of the HB [22]. For this, we introduce multiple scale coordinates $T = \epsilon^2 t$ and $\boldsymbol{X} = \epsilon\boldsymbol{x}$ with $\Delta_{\boldsymbol{X}} \equiv \partial^2_{X_1} + \partial^2_{X_2}$, and expand the densities in powers of ϵ. This yields

$$u(\boldsymbol{x}, t) = \sum_{n=1}^{3} \epsilon^n U^{(n)}(t, T, \boldsymbol{X}) \tag{6}$$

and, similarly, $v = \sum_{n=1}^{3} \epsilon^n V^{(n)}$ and $w = \sum_{n=1}^{3} \epsilon^n W^{(n)}$, where the functions $U^{(n)}, V^{(n)}, W^{(n)}$ are of order $\mathcal{O}(1)$.

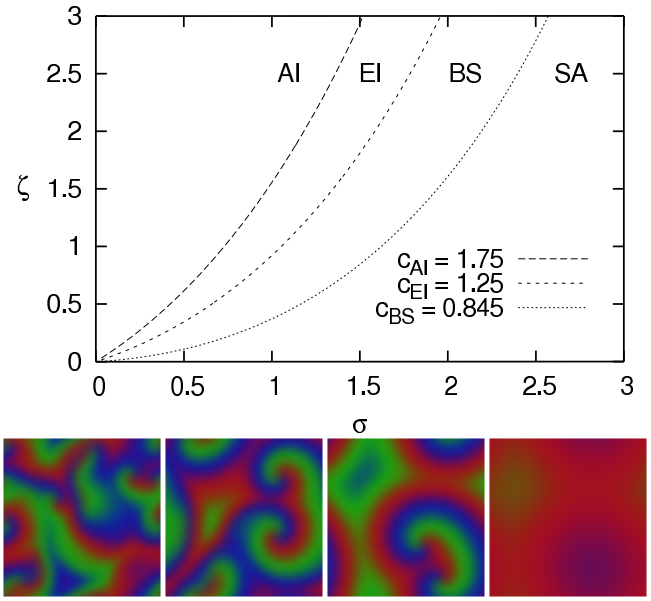

FIG. 2: Upper: System's state diagram around the HB's onset with contours of $c = (c_{AI}, c_{EI}, c_{BS})$ for $\beta = 1$. We distinguish four phases: spiral waves are unstable in AI, EI and SA, whereas they are stable in BS (see text). Lower: Typical snapshots from the PDE (5) in phases AI, EI, BS, SA from left to right (compare with Fig. 1, same parameters used).

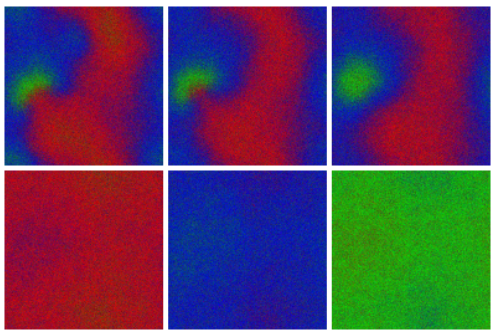

FIG. 3: Typical time evolution of the stochastic system in the SA phase. Same parameters and initial conditions as in Fig. 1 with $\zeta = 0$. Upper: spiral annihilation at different stages, for time $t = (234, 310, 386)$ from left to right. Lower: the oscillatory dominance of each species at $t = (955, 967, 980)$ after relaxation into the homogeneous state (no species extinction).

Substituting (6) into (5) and, using the definition of (u, v, w), we obtain a hierarchy of PDEs and analyze them at each order of ϵ. To obtain a sensible expansion all secular terms are removed. Since the variables u and v are decoupled from w at linear order, one writes $U^{(1)} + iV^{(1)} = \mathcal{A}(T, \boldsymbol{X})e^{i\omega_H t}$, where $\mathcal{A}$ is the complex modulation amplitude. The decoupled equations for w give $W^{(1)} = 0$ and $W^{(2)} \propto |\mathcal{A}|^2$, which is the leading term in the equation for the center manifold [23]. The first secular terms arise at order $\mathcal{O}(\epsilon^3)$ and their removal yields the complex Ginzburg–Landau equation (CGLE) [24] with a real diffusion coefficient δ

$$\partial_T \mathcal{A} = \delta \Delta_{\boldsymbol{X}} \mathcal{A} + \mathcal{A} - (1 + ic)|\mathcal{A}|^2 \mathcal{A}, \qquad (7)$$

where $\delta = \frac{3\beta\delta_E + \sigma\delta_D}{3\beta + \sigma}$ and $\mathcal{A}$ has been rescaled by a constant to give

$$c = \frac{12\zeta(6\beta - \sigma)(\sigma + \zeta) + \sigma^2(24\beta - \sigma)}{3\sqrt{3}\sigma(6\beta + \sigma)(\sigma + 2\zeta)}. \qquad (8)$$

We emphasize that the CGLE (7) has here been *derived perturbatively* and describes the system's dynamics to order ϵ near the HB's onset. This treatment, therefore, differs from that of Refs. [11–13, 16], where a CGLE is obtained by treating heteroclinic cycles as limit cycles.

According to the CGLE (7), the movement in the vicinity of the HB is described by *linear* diffusion, with an effective diffusion constant δ depending on δ_D and δ_E (3). When reproduction dominates over selection ($\beta \gg \sigma$), the lack of empty spaces leads to prevalence of pair-exchanges ($\delta \to \delta_E$), while in the opposite case ($\beta \ll \sigma$), movement occurs mostly via hopping ($\delta \to \delta_D$). As the effective linear diffusive term in (7) affects only the pattern's size, δ can always be rescaled to 1 via $\boldsymbol{x} \to \boldsymbol{x}/\sqrt{\delta}$.

The system state diagram (near the HB) can be inferred from (7) and (8) by referring to the well-known properties of the two-dimensional CGLE [24] and is characterized by four phases with three critical values of c, as illustrated in Fig. 2. In the "spiral annihilation" (SA) phase, when $0 < c < c_{BS}$, the dynamics is characterized by unstable spiraling patterns that collide and vanish. In the "bound state" (BS) regime $c_{BS} < c < c_{EI}$, pairs of stable spirals are formed and coevolve, with their properties described by the CGLE (7). When $c_{EI} < c < c_{AI}$, the spirals become convectively unstable due to the Eckhaus instability (EI) which limits their size and distorts their shape. It is noteworthy that EI has been reported in [12] for a model without mutations ($\mu = 0$). Finally, there is the "absolute instability" (AI) of spiral waves when $c_{AI} < c$, where there are no coherent patterns as the cores are not able to sustain spiral arms. With the explicit values $c_{BS} \approx 0.845$, $c_{EI} \approx 1.25$ and $c_{AI} \approx 1.75$ [24], one obtains the system's state diagram in the $\sigma - \zeta$ plane as shown in Fig. 2. This state diagram sheds light on the results of Fig. 1 where the values $\zeta = (1.8, 1.2, 0.6, 0)$ correspond to $c = (1.9, 1.5, 1.0, 0.6)$, which lie in the four phases AI, EI, BS and SA respectively. A description of the evolution in each phase can be found in the accompanying movies [18]. The phase SA (see Fig. 3), characterized by the annihilation of all spiraling patterns is particularly interesting since it is the only possible phase near the HB's onset when $\zeta = 0$, i.e. for the models of [11, 14] supplemented by mutations. In this phase, spiral annihilation leads to a spatially-homogeneous oscillating state dominated in turn by each species, without any of them going extinct, as described by (4). This

FIG. 4: Influence of mobility on spiraling patterns: typical snapshots in lattice simulations for $(\delta_D, \delta_E) = (0.05, 0.05), (0.20, 0.05)$ from left to right respectively. Other parameters are: $L^2 = 128^2$, $N = 1024$, $\beta = \sigma = 1$, $\zeta = 0.1$ and $\mu = 10^{-6} \ll \mu_H = 0.042$. Geometrically ordered initial conditions, see movies [18] for full details.

deterministic phenomenon is driven by nonlinearity (different from the EI) and not by demographic noise. In the regime $c \ll c_{BS}$, it typically occurs on a short time scale, as illustrated in Fig. 3. This is markedly different from the loss of spiraling patterns driven by noise after a time growing exponentially with the system size as found in [11, 14].

Our analysis in terms of the CGLE (7) relies on a perturbative treatment around the onset of HB where $\epsilon \ll 1$, but is found to faithfully describe the system's properties far from the HB. For instance, when $\beta = \sigma = 1$ and $\zeta = 0$ ($\mu_H = 0.042$), the system is still in the SA phase even for $\mu = 0.02$ ($\epsilon = 0.25$) as predicted by our theory (see Figs. 1 and 3). We have also checked that our analysis is robust against simultaneous random perturbations (up to $\pm 5\%$) of all the reaction rates (1)-(3) [20]. As shown in Figs. 1 and 2, the PDEs (5) describe perfectly the stochastic metapopulation model when $N \gg 1$ and, in practice, are still accurate when $N \gtrsim 16$ for any nonzero mobility. Furthermore, when $N = 2$ and the mobility rates are sufficiently high, as discussed in [11], the state diagram of Fig. 2 is still valid [18].

Away from the HB's onset (e.g. for $\mu = 10^{-6}$) and when $\delta_D \neq \delta_E$, the stability of spirals is affected by the nonlinear diffusive terms of (5). In fact, when noise is negligible ($N \gg 1$), one observes a far-field break-up of the spiraling patterns caused by nonlinear mobility, as shown in Fig. 4 and [18].

In summary, we have investigated the stability of spiraling patterns in a generic three-species model whose evolution results from the combined effects of cyclic dominance, mutation and biologically-motivated nonlinear mobility. Inspired by recent experiments [7], we have developed a metapopulation description and analyzed the dynamics in terms of a CGLE derived via a multiscale expansion around the Hopf bifurcation's onset. We have thus obtained the system's state diagram, which is characterized by four phases, with only one capable of supporting stable spiraling patterns. The instabilities in the three other phases are not driven by noise. In particular, we have identified a phase (SA) where spirals annihilate, leading to spatially uniform dominance of each species in turn. Importantly, these behaviors, which arise in a wide region of the parameter space around the Hopf bifurcation, are robust and *independent* of the mobility rates. This is in stark contrast with the results of Refs. [11, 12, 14], where spiraling patterns and spatial uniformity were respectively found at low and high mobility, and may explain why spiraling patterns turn out to be elusive in the microbial experiments of Refs. [6, 7]. Additionally, regardless of internal noise, we show that nonlinear diffusion causes far-field break-up of spiral waves away from the Hopf bifurcation's onset.

The authors acknowledge discussions with Tobias Galla at an early stage of this project. BS is grateful for support of an EPSRC studentship.

* Electronic address: mmbs@leeds.ac.uk
† Electronic address: M.Mobilia@leeds.ac.uk
‡ Electronic address: A.M.Rucklidge@leeds.ac.uk

[1] S. A. Levin and L. A. Segel, Nature (London) **259**, 659 (1976); M. P. Hassel, H. N. Comins and R. M. May, *ibid* **370**, 290 (1994); E. R. Abraham, *ibid* **391**, 577 (1998); J. L. Maron and S. Harrison, Science **278**, 1619 (1997).

[2] J. B. C. Jackson and L. Buss, Proc. Natl. Acad. Sci. U.S.A. **72**, 5160 (1975); B. Sinervo and C.M. Lively, Nature (London) **380**, 240 (1996); B. C. Kirkup and M. A. Riley, *ibid.* 428, 412 (2004).

[3] A.???M. Turing, Phil. Trans. R. Soc. B **237**, 37 (1952).

[4] C. A. Lugo and A. J. McKane, Phys. Rev. E **78**, 051911 (2008); T. Butler and N. Goldenfeld, Phys. Rev. E **80**, 030902(R) (2009); *ibid.* **84**, 011112 (2011).

[5] E. Pennisi, Science **309**, 93 (2005); W. Thuiller, Nature 448, 550 (2007).

[6] B. Kerr, M. A. Riley, M. W. Feldman and B. J. M. Bohannan, Nature (London) **418**, 171 (2002).

[7] B. Kerr, C. Neuhauser, B. J. M. Bohannan, A. M. Dean, Nature **442**, 75 (2006); J. R. Nahum, B. N. Harding, and B. Kerr, Proc. Natl. Acad. Sci. U.S.A. **108**, 10831 (2011).

[8] J. Hofbauer and K. Sigmund, *Evolutionary games and population dynamics* (Cambridge University Press, 1998); G. Szabó, Phys. Rep. **446**, 97 (2007); E. Frey, Physica A **389**, 4265 (2010).

[9] T. Reichenbach, M. Mobilia and E. Frey, Phys. Rev. E **74**, 051907 (2006); M. Berr, T. Reichenbach, M. Schottenloher and E. Frey, Phys. Rev. Lett. **102**, 048102 (2009); M. Mobilia, J. Theor. Biol. **264**, 1 (2010); A. P. O. Müller and J. A. C. Gallas, Phys. Rev. E **82**, 052901 (2010).

[10] K. I. Tainaka, Phys. Rev. Lett. **63**, 2688 (1989); Phys. Rev. E **50**, 3401 (1994); L. Frachebourg, P. L. Krapivsky and E. Ben-Naim, Phys. Rev. Lett. **77**, 2125 (1996); G. Szabó and A. Szolnoki, Phys. Rev. E **65**, 036115 (2002); G. Szabó, A. Szolnoki and R. Izsák, J. Phys. A. Math. Gen. **37**, 2599 (2004); M. Perc, A. Szolnoki and G. Szabó, *ibid.* **75**, 052102 (2007); Q. He, M. Mobilia and U. C. Täuber, Phys. Rev. E **82**, 051909 (2010); X. Ni, W. X. Wang, Y. C. Lai, and C. Grebogi, Phys. Rev. E **82**, 066211 (2010).

[11] T. Reichenbach, M. Mobilia and E. Frey, Nature (Lon-

don) **448**, 1046 (2007); Phys. Rev. Lett. **99**, 238105 (2007); J. Theor. Biol. **254**, 368 (2008).
[12] T. Reichenbach and E. Frey, Phys. Rev. Lett. **101**, 058102 (2008).
[13] M. Peltomäki and M. Alava, Phys. Rev. E **78**, 031906 (2008).
[14] Q. He, M. Mobilia and U. C. Täuber, Eur. Phys. J. B **82**, 97 (2011); Q. He, U. C. Täuber and R. K. P. Zia, *ibid.* **85**, 141 (2012).
[15] R. M. May and W. J. Leonard SIAM J. Appl. Math. **29**, 243 (1975).
[16] J. Cremer, MSc Thesis (Ludwig-Maximilians-Universität München, 2007).
[17] R. Levins, Bull. Entomol. Soc. Am. 15, 237 (1969); I. Hanski, *Metapopulation Ecology* (New York, Oxford University Press, 1999).
[18] B. Szczesny, M. Mobilia and A. M. Rucklidge, doi: 10.6084/m9.figshare.96949
[19] D. B. Kearns, Nature Rev. Micro. **8**, 634 (2010).
[20] B. Szczesny, M. Mobilia and A. M. Rucklidge, in preparation
[21] N. G. Van Kampen, *Stochastic Processes in Physics and Chemistry* (Elsevier, 2007); C. Gardiner, *Stochastic Methods* (Springer, 2010).
[22] P. Miller, *Applied Asymptotic Analysis, Graduate Studies in Mathematics* (American Mathematical Society, 2006).
[23] J. Guckenheimer and P. Holmes, *Nonlinear Oscillations, Dynamical Systems, and Bifurcations of Vector Fields* (Springer, 1983).
[24] I. S. Aranson, L. Kramer and A. Weber, Phys. Rev. E **47**, 3231 (1993); I. S. Aranson and L. Kramer, Rev. Mod. Phys. **74**, 99-143 (2002).